Proceedings of the Seventh International Conference on
Railway Technology: Research, Development and Maintenance
Edited by: J. Pombo
Civil-Comp Conferences, Volume 15, Paper 11.4
Civil-Comp Press, Edinburgh, United Kingdom, 2026
ISSN: 2753-3239, doi: 10.4203/ccc.15.11.4

Study on the Influence of Different Natural Vibration Frequencies of Track Beams on the Vehicle-Bridge Coupling Dynamics of High-Speed Maglev

J. Yang and G. Lin

National Maglev Transportation Engineering R&D Center, Shanghai, China

Abstract

To investigate the influence characteristics of the natural vibration frequency of track beams on high-speed maglev dynamics, a high-speed maglev vehicle-bridge coupling dynamic model is established, and the influence law of the natural vibration frequency of track beams on the dynamic response characteristics of high-speed maglev under different speeds is analyzed. The research results show that the coefficient 1.1 in the first-order frequency formula is a vehicle dynamics correction factor, which inhibits the extreme fluctuation of the levitation electromagnetic force to a certain extent and reduces the fluctuation range of the electromagnetic force. However, the difference magnitude is small; neglecting the coefficient 1.1 does not cause system instability or resonance risk, and it is essentially a conservative design for the dynamic coupling excitation between the track beam and the suspension system.

Key words: high-speed maglev; vehicle-bridge coupling; dynamic characteristics; track beam’s natural vibration frequency

1. Introduction

The first-order frequency of the track beam is one of its most important inherent dynamic characteristics. It fundamentally determines the dynamic response behavior of the bridge under the moving train load and exerts a profound influence on the dynamic performance of the vehicle system, constituting a typical core issue of the coupled dynamic interaction among vehicle, bridge and track beam, and directly governing the operational safety, running stability and ride comfort of high-speed trains.

Zhao et al. [1] investigated the dynamic response of the vehicle system considering the vertical vehicle-bridge coupling effect. Ren et al. [2] established a vertical vehicle-track-bridge coupling dynamic model for medium-low speed maglev trains considering the flexibility of F-rail and bridge on the ANSYS software platform, and investigated the vibration response of the vehicle-bridge system at a speed of 80 km/h. Zhu et al. [Error! Reference source not found.] simulated the action of maglev vehicles with moving loads, and analyzed the dynamic responses of the bridge under working conditions such as different train speeds and different bridge damping ratios. Wang et al. [3] adopted the numerical analysis method to investigate the dynamic response of the vehicle-bridge coupling system when a high-speed maglev train passes through a simply supported girder bridge, and the results show that the vertical vibration acceleration of the bridge is one of the control indices for the running safety of maglev trains. Han et al. [4] adopted the Euler-Bernoulli bridge model to analyze the instability of vehicle-track coupled vibration induced by control parameters, and investigated the influence of different structural parameters of track beams on the vehicle-track coupled vibration of medium-low speed maglev trains. Yu H [6] combined with the track beam of the Shanghai maglev system, conducted finite element simulation of maglev trains crossing bridges to analyze the dynamic response law of the vehicle-bridge system during bridge crossing, and pointed out that the stiffness of the track beam has a significant influence on the dynamic response of the vehicle system.

For the German high-speed maglev railway, the requirement for the vertical deflection of the track beam is specified as $\le L/(4000 \sim 4800)$ for vertical deflection. It can be seen that the stiffness requirement for the track beam of maglev lines is more stringent than that of conventional high-speed railways. Coupled resonance may occur when a maglev passes. Therefore, the first-order natural frequency of the beam should be strictly controlled in the design of maglev track beams. The *Design Code for German Maglev Lines* [Error! Reference source not found.] stipulates that the fundamental natural frequency of the track beam shall satisfy the following requirement:

$$f_{n.1} \ge 1.1 v / L_n \tag{1}$$

Where $f_{n.1}$ is the first-order natural frequency of the track beam, in Hz; v is the maximum operating speed of the maglev passing through the track beam, in m/s; L_n is the span length of the track beam.

Since the maglev-track contact relationship is essentially different from the wheel-rail contact relationship in high-speed railways, the vehicle-track coupled vibration of wheel-rail systems may be excited at the same frequency, while that of maglev-track beam systems may not be induced. Thus, the inclusion of the coefficient 1.1 may render the design of track beams overly conservative. It is therefore necessary to consider the effects caused by vehicle-track coupled vibration in the structural design of track beams. To this end, a comprehensive dynamic model for the high-speed maglev vehicle-track beam coupling system is established in this paper, and the dynamic responses of the bridge as well as the vehicle dynamic responses under different operating speeds are investigated with the flexibility of the track beam taken into account.

2. Dynamic model for vehicle-track beam coupling of high-speed maglev

2.1 The control model of the suspension system

The maglev-track interaction model reflects the relationship between electromagnetic force and gap, coil current and various material parameters. Most existing studies adopt the classical one-dimensional analytical formula for electromagnetic force [Error! Reference source not found.], which describes a relationship where the electromagnetic force is directly proportional to the square of the coil current and inversely proportional to the square of the levitation gap:

$$F_m = \frac{\mu_0 N^2 A}{4}\left(\frac{I(t)}{z(t)}\right)^2 \tag{2}$$

Where N is the number of coil turns; A is the effective area of the coil, m²; μ_0 is the vacuum permeability; I is the coil current, A; $z(t)$ is the levitation air gap, m.

In this paper, a two-stage series-connected suspension control system is adopted with reference to relevant literature [Error! Reference source not found.], the structure of which is shown in Fig. 1. In the electromagnetic force calculation/control system, the vertical displacement and acceleration of the levitation electromagnet obtained from the dynamic system simulation are input into the control system. The control voltage is derived through the calculation of the state observer and the control system, and then input into **Eq.** $F_m = \frac{\mu_0 N^2 A}{4}\left(\frac{I(t)}{z(t)}\right)^2$ (2) together with the vertical displacement of the levitation electromagnet; the levitation force is subsequently obtained and output via calculation.

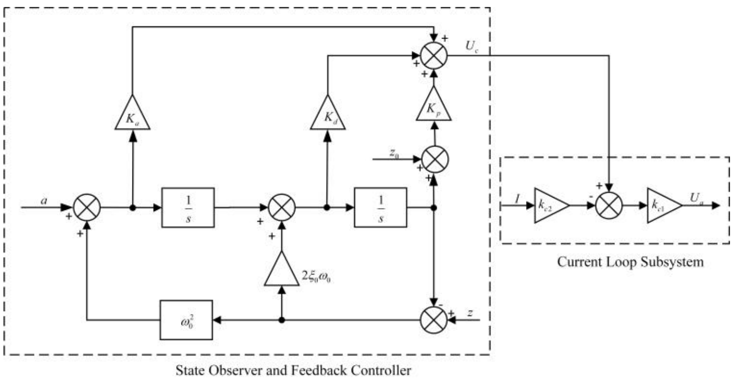

Fig. 1 control system structure

2.2 The model of track beam

A simply supported concrete beam with a standard span of 24.768 m is recommended for the standard simply supported beam of the Shanghai High-Speed Maglev Line. The beam height is 2.2 m, and the slab thickness at the general sections is 300 mm. Within the range of the beam end supports, the cross-section is different from that at the mid-span. The cross-sections at the mid-span and supports [Error! Reference source not found.] are shown in Fig. 2, with the unit in millimeters (mm).

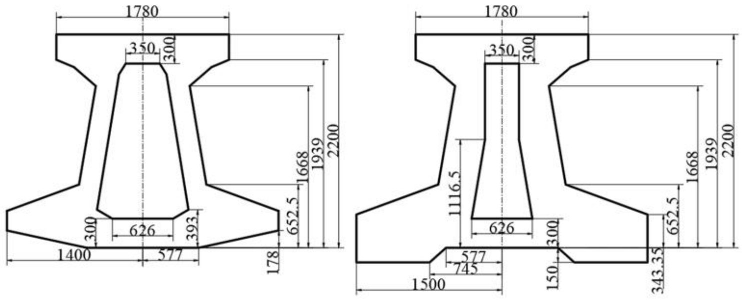

(a) mid-span section **(b) support section**

Fig. 2 Schematic of the track beam structure

The most prevalent simply supported single-span beam on the Shanghai High-Speed Maglev Line is adopted as the simulation subject in this study. The Bernoulli-Euler beam equation, which is widely adopted in the research of maglev systems, is employed for the track beam model:

$$EI\frac{\partial^4 h(x,t)}{\partial x^4}+c\frac{\partial h(x,t)}{\partial t}+\rho A\frac{\partial^2 h(x,t)}{\partial t^2}=F_m(x,t)+F_h(x,t) \tag{3}$$

Where h is the dynamic deflection of the track beam in the Z-direction; EI is the flexural rigidity; c is the track damping; ρ is the linear mass density of the track beam; $F_m(x,t)$ is the electromagnetic force exerted on the track beam by the electromagnet; $F_h(x,t)$ is the support force acting on the track beam by the bearing.

The finite element model and mesh generation of the track beam are shown in Fig. 3.

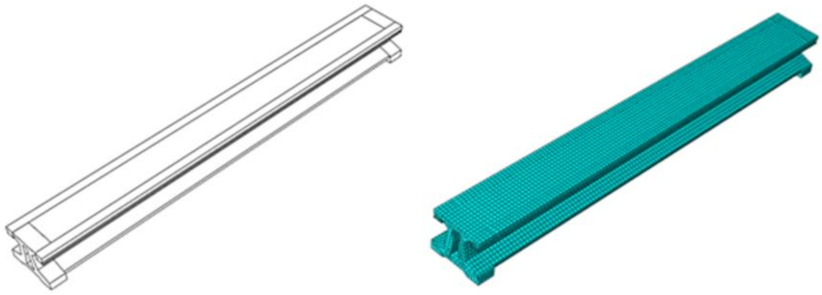

(a) geometric structure **(b) mesh generation**

Fig. 3 Finite element model and mesh generation of the track beam

Based on the Euler-Bernoulli beam theory and **Eq.** $f_{n.1} \geq 1.1v / L_n$ (1), the general formula for the first-order natural frequency of a simply supported beam with uniform cross-section, length L and uniformly distributed mass of linear density μ at both ends is given as follows:

$$f_1 = \frac{\pi}{2L^2}\sqrt{\frac{EI}{\rho A}} \tag{4}$$

In this paper, E is taken as 3.55×10^6 Pa; I as 0.5 m^4; L is taken as 24.768 m; A denotes the cross-sectional area with a value of 1.78 m^2.

Based on **Eq.** $f_{n.1} \geq 1.1v / L_n$ (1) and $f_1 = \frac{\pi}{2L^2}\sqrt{\frac{EI}{\rho A}}$ (4), the mass of the track beam must be less than a certain upper limit:

$$m \leq \frac{\pi EI}{4.84L^2v^2} \tag{5}$$

If the coefficient 1.1 in **Eq.** $f_{n.1} \geq 1.1v / L_n$ (1) is neglected, the upper limit of the track beam mass is:

$$m \leq \frac{\pi EI}{4L^2v^2} \tag{6}$$

2.3 The rigid-flexible coupled dynamics model of high-speed maglev

The rigid-flexible coupled dynamics model of high-speed maglev is shown in Fig. 4, which is composed of one body and six groups of suspension frames, supporting the body by four air springs. There are six pairs of suspension electromagnets and six pairs of guidance electromagnets in total. The body and suspension frame both take 6 degrees of freedom, i.e. longitudinal, lateral, vertical, roll, pitch and yaw; The levitation electromagnet's vertical and pitch DOF are considered in the model due to its action of providing the vertical electromagnetic force. Similarly, the guidance electromagnet's lateral and yaw DOF are considered, all shown in Table 1. The vehicle's body, suspension frame, levitation electromagnet and guidance electromagnet are equivalent to rigid bodies, and the suspension components such as electromagnetic force and air spring are simplified to force elements. Notably, the track beam is modeled as a flexible body to establish a rigid-flexible coupled model of the vehicle and track beam. The vehicle system dynamics model is built according to the connection relationship between components, in which the vehicle's working height is set at 10 mm.

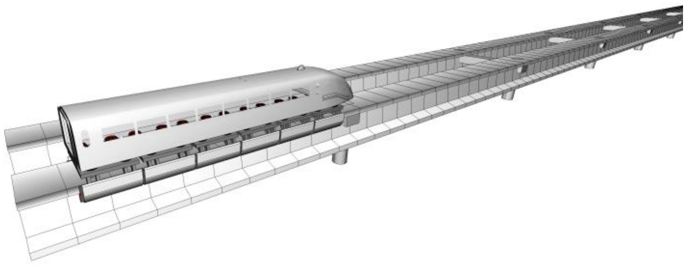

Fig. 4 Dynamic model of high-speed maglev vehicle–track beam

Table 1 Vehicle's DOF

DOF	longitudinal	lateral	vertical	roll	pitch	yaw
Body	√	√	√	√	√	√
Suspension Frame	√	√	√	√	√	√
Levtiation electromagnet	/	/	√	/	√	/
Guidance electromagnet	/	√	/	/	/	√

By inverting the irregularity in the time domain, the time domain's form can be obtained, which can effectively simulate the guideway surface's irregularity. In this paper, the irregularity spectrum can effectively reflect long wave signals. The amplitude of vertical irregularity fluctuates within ± 4 mm, while the lateral irregularity fluctuates within ± 3 mm.

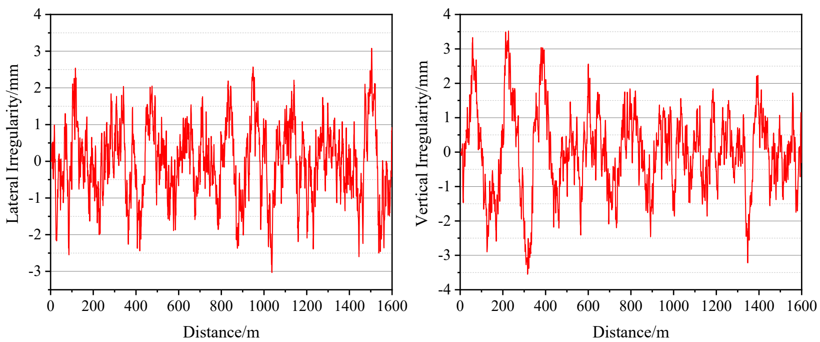

(a) lateral irregularity **(b) vertical irregularity**

Fig. 5 Track irregularity amplitude

3. Analysis of high-speed maglev's vehicle–track beam coupled dynamic performance

3.1 Riding comfort index

Since there is no specific evaluation index for the stability of maglev, wheel rail vehicles' can be used for reference due to the reason that the stability mainly focuses on the ride quality of vehicles. According to "Code for Design of High-Speed Railway TB 10621-2014"[11] and "Specification for Dynamic Performance Assessment and Testing Verification of Rolling Stock GB/T 5599-2019"[12], and with reference to the evaluation criteria adopted in previous speed increase tests, Sperling index is used to judge the running stability and UIC 518:2009[13] for ride comfort. The acceleration measuring points set in accordance with GB/T 5599 are shown in Fig. 6. The evaluation indexes of vehicle stability mainly include lateral stability, vertical stability and ride comfort. The evaluation grades are shown from Table 3 to Table 4. According to the GB/T 5599, the calculation method of stability index *W* is:

$$W = 3.57\sqrt[10]{\frac{A^3}{f} / F(f)} \tag{7}$$

Where *A* is the vibration acceleration, *m/s²*; *f* is the vibration frequency, *Hz*; *F(f)* is the frequency correction factor.

Table 2 Correction factor table [12]

Vertical vibration		Lateral vibration	
f / Hz	$F(f)$	f / Hz	$F(f)$
$0.5 \le f < 5.9$	$0.325 f^2$	$0.5 \le f < 5.4$	$0.8 f^2$
$5.9 \le f < 20$	$400 / f^2$	$5.4 \le f < 26$	$650 / f^2$
$f > 20$	1	$f > 26$	1

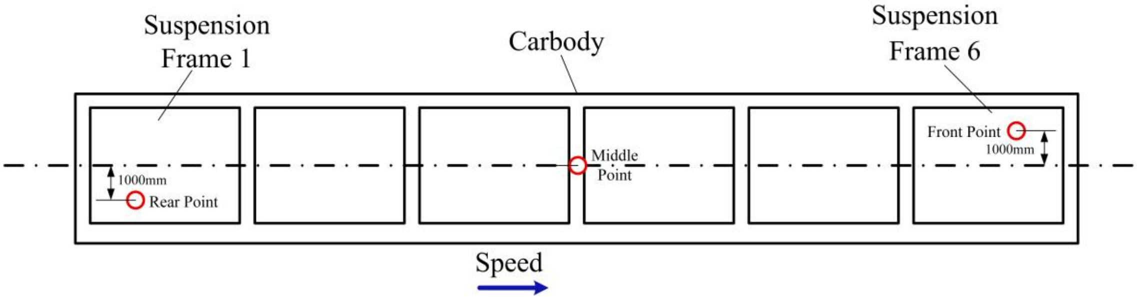

Fig. 6 Acceleration measurement point.

Table 3 Riding evaluation index of passenger cars and EMUs [12]

Riding level	Riding index *W*	Evaluation
Grade 1	$W \le 2.50$	Excellent
Grade 2	$2.50 < W \le 2.75$	Good
Grade 3	$2.75 < W \le 3.00$	Qualified

Table 4 Comfort index of passenger cars and EMUs [13]

Comfort level	Comfort index	Evaluation
Excellent	*N*MV <1	Very comfortable
Good	1< *N*MV <2	Comfortable
General	2< *N*MV <4	Average comfortable
Poor	4< *N*MV <5	Uncomfortable
Fail	*N*MV >5	Extremely uncomfortable

The following part will analyze in detail the dynamic response of the high-speed maglev coupling system under different speed conditions, with the focus on vehicle riding indicators, including acceleration, comfort, vertical acceleration of the levitation electromagnet, levitation force and levitation gap. Among them, the riding index selects measurement points at the front, middle and rear of the vehicle.

3.2 Dynamic response of track beam

To investigate the necessity of the coefficient of 1.1 in the formula for calculating the first-order natural frequency of track beam, a rigid-flexible coupled dynamic simulation analysis of the high-speed maglev vehicle- track beam is conducted in this section by using two different models. One model incorporates the coefficient of 1.1 (abbreviated as ***1.1v/l***) while the other excludes it (abbreviated as ***v/l***), aiming to verify whether the resonance will occur between the vehicle and the track beam when the vehicle speed reaches the critical speed corresponding to the track beam's first-order natural frequency. Two speed conditions are considered in the simulation: 300 km/h, the operational speed of the Shanghai maglev line, and 600 km/h, the expected operational speed of high-speed maglev systems. Based on Eq. $m \le \frac{\pi EI}{4.84L^2v^2}$ (5 $m \le \frac{\pi EI}{4L^2v^2}$ (6), the ultimate mass of the track beam at various speeds can be derived.

This section presents the time histories of the vertical acceleration and vertical deflection of the 50th track beam under varying vehicle speeds as the vehicle passes, shown in Fig. 7. It can be seen from the figure that the vertical acceleration and deflection of the track beam increase with the rise of vehicle speed. Meanwhile, as the vehicle speed increases, the time for the vehicle to pass the flexible beam is shortened, meaning the duration of the vehicle's action on the track beam decreases. Consequently, the vertical dynamic deflection at the span of the track beam reduces accordingly.

At the same speed, the peak values of acceleration and deflection without considering the 1.1 coefficient are slightly higher than those considering the 1.1 coefficient. However, the amplitude does not show a significant increase, and no residual deformation is observed, indicating that the 1.1 coefficient does not have a substantial impact on the vertical deformation of the track beam. Furthermore, under the speed of 600 km/h, the peak values of both indicators are significantly higher than those under the speed of 300 km/h condition, reflecting the amplification effect of high-speed operation on the dynamic response of the track beam. This indicates that the speed is a core factor determining the magnitude of the vertical deflection response of the track beam, suggesting that the 1.1-times frequency safety coefficient specified in the current code may be redundant.

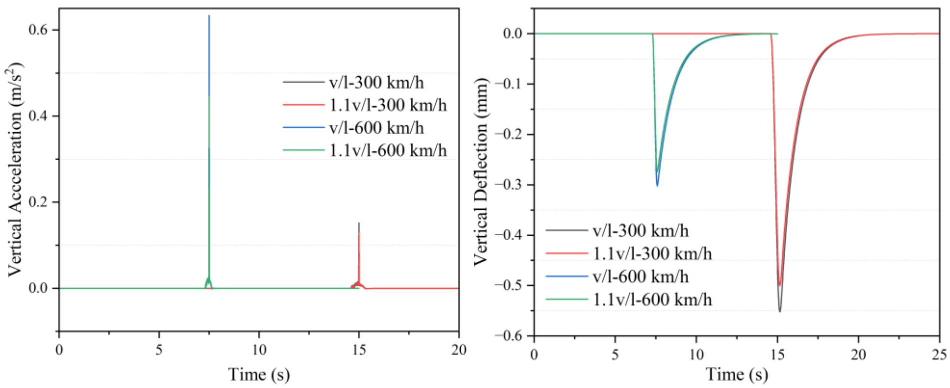

(a) vertical acceleration **(b) vertical deflection**

Fig. 7 Dynamic response of the 50th track beam

3.3 Dynamic response of vehicle

For the analysis of maglev's dynamic response, the acceleration response of the vehicle is extracted from the front measuring point of the leading car body, and the dynamic characteristics of the levitation gap and levitation force of the levitation electromagnet are obtained from the front measuring point on the left side of the second levitation module at the front of the leading car.

3.3.1 300 km/h

The front, middle and rear riding index of the maglev calculated based on two models are given by Fig. 8, where (a) is the lateral and vertical index and (b) is the comfort index.

First, the riding indices are analyzed. The left vertical axis in the figure represents the lateral riding index and the right vertical axis represents the vertical one. It can be seen that the introduction of the coefficient of 1.1 leads to an overall decrease in both lateral and vertical index. This indicates that in the current vehicle-track beam coupling system model, the first-order natural frequency calculated with the coefficient of 1.1 enables the evaluation points of the system to avoid an adverse resonance region, thus yielding a more optimal prediction of dynamic performance with smaller values. The coefficient exerts a significantly greater influence on the vertical riding than on the lateral one. At the front of the vehicle, the vertical index is reduced by approximately 13.0%, while the lateral index is only decreased by about 1.4%, which demonstrates that the correction effect of the coefficient of 1.1 is more closely correlated with the vertical dynamic characteristics of the system.

Consistent with the conclusions of the riding index, after introducing the coefficient of 1.1, the comfort indices at all positions show a systematic decrease, indicating that this coefficient has a consistent optimizing effect on the prediction of overall ride quality. It is noteworthy that at the front of the vehicle, the comfort indices from both models exceed the optimal value of 2, indicating that this position is the least comfortable in terms of ride comfort. The comfort index at the front shows the most significant reduction in the model considering the coefficient of 1.1, with a decrease of approximately 8.3%, while the reduction at the middle is the smallest. This suggests that in regions with poorer system dynamic performance, improving the track beam characteristic frequency has a slightly sensitive effect on enhancing the riding index, whereas its influence is relatively minor in positions where comfort is already optimal.

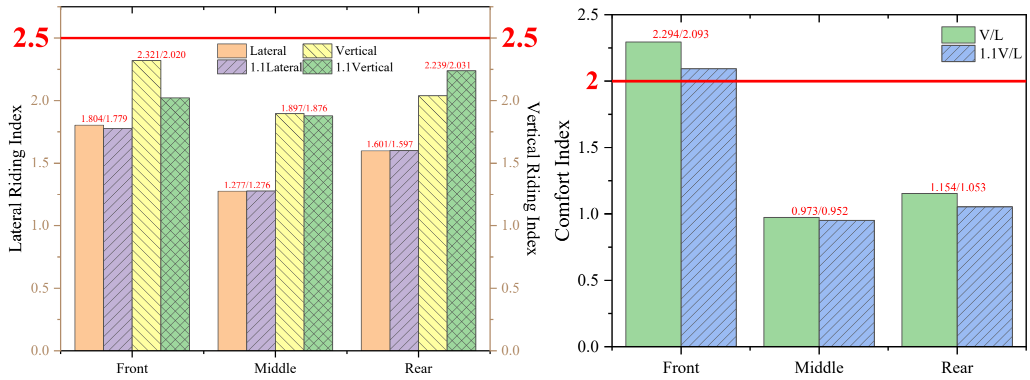

(a) lateral and vertical riding index **(b) comfort index**

Fig. 8 Vehicle's riding index

The vertical acceleration of the maglev calculated based on two models are given by Fig. 9. It can be seen from figure that the overall fluctuation trends of the two curves are consistent, indicating that the dominant vibration modes of the system are governed by the same physical mechanisms. Furthermore, the results without considering the coefficient of 1.1 do not exhibit anomalous values, suggesting that the system response does not display significant resonant characteristics. However, during most periods, the amplitude of the acceleration response calculated with the coefficient of 1.1 is markedly lower than that without it. This directly corresponds to the conclusion from the riding index that "the results of the model considering the coefficient of 1.1 are lower," visually verifying that the introduction of the coefficient 1.1 reduces the overall vibration intensity of the system in the time domain.

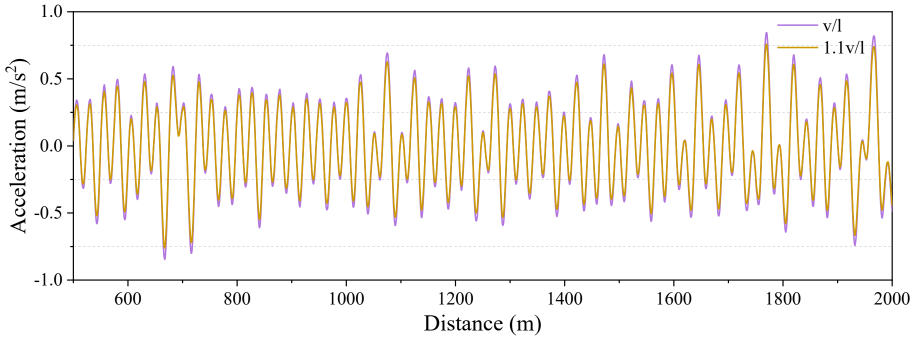

Fig. 9 Vehicle's vertical acceleration

The levitation gap of the levitation electromagnet calculated based on two models are given by Fig. 10. It can be seen from the figure that the levitation gap of both models exhibits favorable fluctuation stability, consistently oscillating around the rated gap of 10 mm. The fluctuation range of the model considering the coefficient of 1.1 remains stable within the interval of 9.8 mm to 10.1 mm. In contrast, the fluctuation amplitude of the model without considering the coefficient of 1.1 increases significantly, reaching a maximum fluctuation of 10.2 mm, with a noticeably higher occurrence of high-frequency fluctuations. However, no extreme fluctuations exceeding the engineering tolerance threshold are observed. This phenomenon indicates that the 1.1 frequency amplification factor of the track beam's first-order frequency alters the dynamic coupling relationship between the track beam and the levitation electromagnet to some extent. Reducing the characteristic frequency of the track beam makes the vibrational excitation from the track beam more easily transmitted to the levitation gap, thereby inducing more pronounced gap fluctuations and reducing the stability of the levitation system.

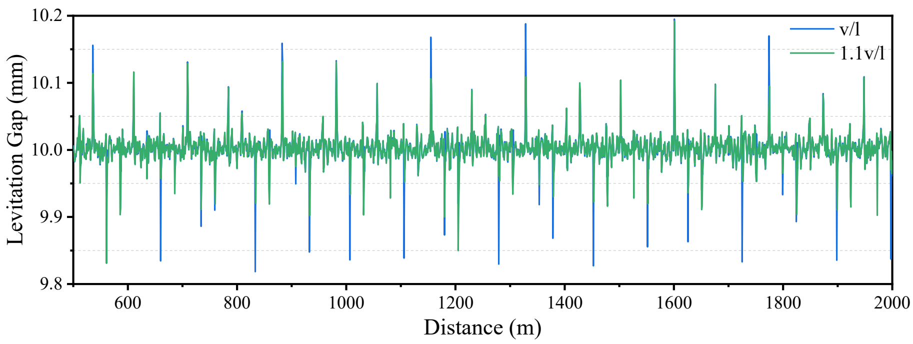

Fig. 10 Levitation electromagnet's levitation gap

The levitation force of the levitation electromagnet calculated based on two models are given by Fig. 11. It can be seen from the figure that when the coefficient of 1.1 is not considered, the levitation electromagnetic force fluctuates within a range of 14 kN to 27 kN, exhibiting relatively large amplitude fluctuations. Multiple instances of sharp drops and sudden rises are observed, reflecting stronger volatility in the system's dynamic response. In contrast, when the coefficient of 1.1 is considered, the fluctuation range of the levitation electromagnetic force decreases to 17 kN to 21 kN, with a significant reduction in overall fluctuation amplitude and no extreme large-scale oscillations, indicating a notable improvement in the smoothness of the dynamic response. This suggests that the first-order natural frequency of the track beam without considering the coefficient of 1.1 is closer to the excitation frequency during train operation. Such frequency matching enhances the dynamic coupling between the track beam and the levitation electromagnet, making the vibrational excitation from the track beam more easily transmitted to the levitation system. This leads to resonant fluctuations in the electromagnetic force, manifested as peaks and troughs in its waveform. However, this difference does not lead to the system instability or pose any resonance risk.

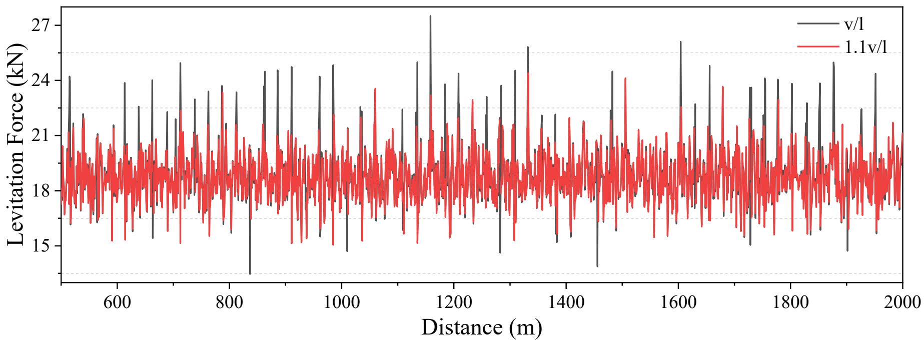

Fig. 11 Levitation electromagnet's levitation force

3.3.2 600 km/h

The front, middle and rear riding index of the maglev calculated based on two models are given by Fig. 12, where (a) is the lateral and vertical riding index and (b) is the comfort index.

The study of lateral and vertical riding index reveals that after applying the coefficient of 1.1, the indices for the front, middle, and rear of the vehicle all show a consistent decrease, with reductions ranging between 0.08 and 0.11. It is noteworthy that increasing the first-order frequency of the track beam provides a greater safety margin for the vertical riding index, which is originally close to the *EXCELLENT* threshold of 2.5. Compared to the results of 300 km/h, the optimization effect achieved by applying the coefficient of 1.1 at 600 km/h is more significant, resulting in a larger reduction in the riding indices.

Analysis of the comfort index reveals that the overall variation trend is similar to that observed under the speed of 300 km/h. Although the front index of the vehicle has exceeded the excellent threshold, the consideration of the 1.1 coefficient significantly mitigates the deterioration trend in comfort. By examining the reduction rate of the index, it can be observed that the magnitude of reduction for each index under the 600 km/h condition is greater than that under the 300 km/h condition.

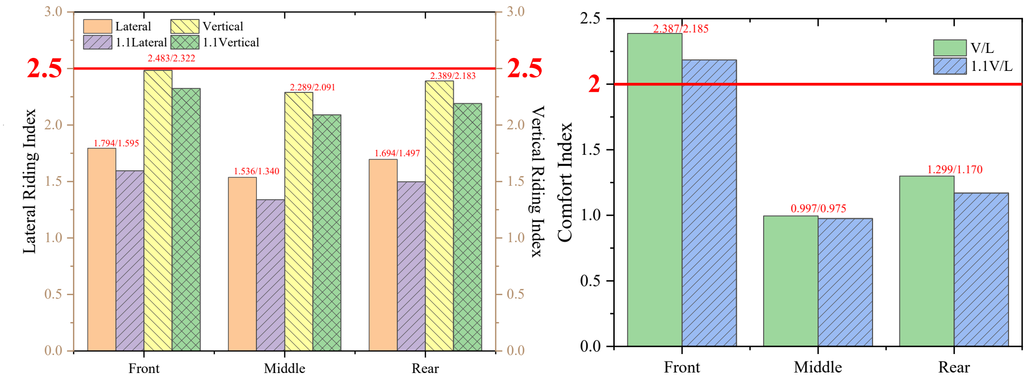

(a) lateral and vertical riding index **(b) comfort index**

Fig. 12 Vehicle's riding index

The vertical acceleration of the maglev calculated based on two models are given by Fig. 13. It can be seen from figure that the overall fluctuation trends of two curves remain consistent, and the inclusion of the coefficient 1.1 helps to suppress the vertical vibration response of the vehicle to some extent. Compared with the results of 300 km/h, the difference that the acceleration amplitude of the model without the 1.1 coefficient is significantly larger than that of the model with the coefficient is more pronounced, and a noticeable discrepancy exists in the range of acceleration fluctuations. This phenomenon indicates that the dynamic coupling between the track beam and the levitation system is stronger under high-speed conditions. However, this difference does not lead to the system instability or resonance risk.

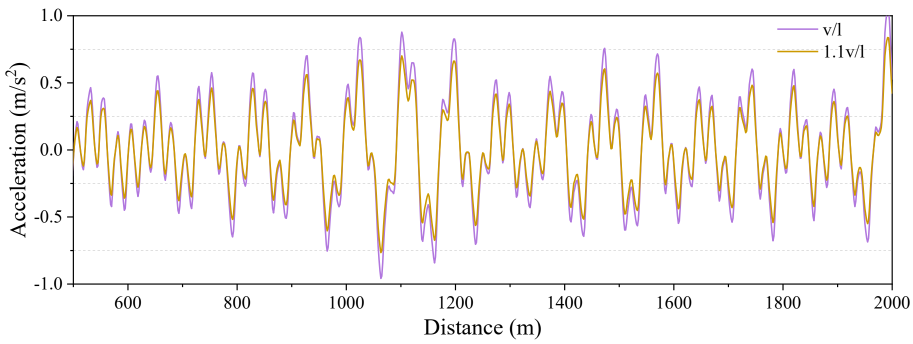

Fig. 13 Vehicle's vertical acceleration

The levitation gap of the levitation electromagnet calculated based on two models are given by Fig. 14. It can be seen from the figure that the fluctuation range of the levitation gap remains stable within 10±2 mm and is moderately wider compared to the results at 300 km/h. Analyzing the effect of the coefficient 1.1 at different speeds reveals that at 300 km/h, the difference between two models is relatively small except for a few peaks and troughs, whereas at 600 km/h, the difference becomes more pronounced, albeit still a minor difference of approximately 0.2 mm. The inclusion of the coefficient 1.1 slightly optimizes the peak values of the gap fluctuation but does not significantly improve the system stability.

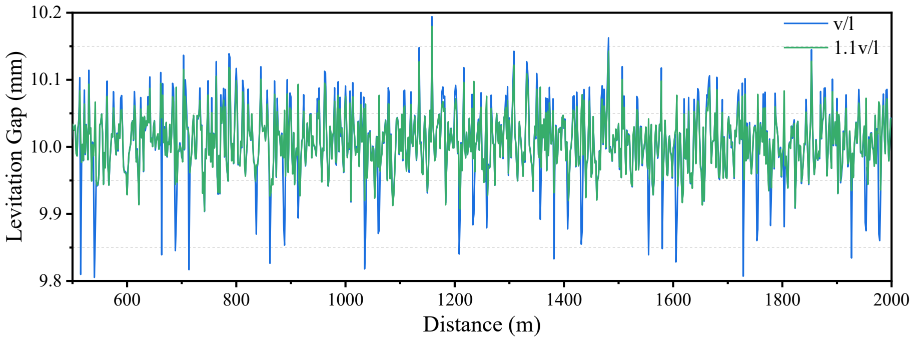

Fig. 14 Levitation electromagnet's levitation gap

The levitation force of the levitation electromagnet calculated based on two models are given by Fig. 15. It can be seen from the figure that at the speed of 600 km/h, the fluctuation range of the levitation force expands to 12 kN~26 kN, which is slightly larger than the range of 14 kN~21 kN observed at 300 km/h. Compared to the results at 300 km/h, the difference between two models at 600 km/h becomes more pronounced. The results without considering the 1.1 coefficient exhibit a larger fluctuation range and increased extreme fluctuations relative to those with the coefficient, but the difference remains within 2 kN and does not substantially affect the system stability.

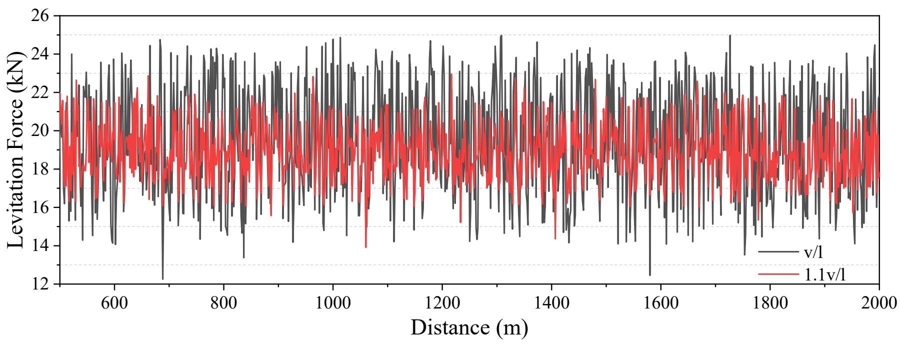

Fig. 15 Levitation electromagnet's levitation force

4. Conclusions

Based on the studies mentioned above, conclusions can be drawn as follows: The coefficient 1.1 in Eq. $f_{n.1} \geq 1.1v / L_n$ (1) serves as a dynamic correction factor, which partially suppresses extreme fluctuations in the electromagnetic levitation force and reduces its oscillation range. Systematically, it lowers the predicted values of both lateral and vertical riding indices of the vehicle, with a more pronounced improvement predicted for vertical dynamic performance compared to lateral performance. This effect becomes increasingly significant at higher speeds. However, the magnitude of the difference is negligible, posing no risk of system instability or resonance. Fundamentally, this factor embodies a conservative design intended to mitigate the dynamic coupling excitation between the track beam and levitation system.

5. References

1. Zhao, C., Zhai, W., & Cai, C. Study on vertical coupling dynamics of maglev vehicle/guideway. Journal of the China Railway Society, 23(5), 27–33, 2001.
2. Ren, X., Zhao, C., Feng, X., et al. Simulation analysis of vertical coupled vibration of medium-low speed maglev vehicle-track-bridge system. Railway Standard Design, 63(2), 70–76, 2019.
3. Zhu, Z., Hu, M., Feng, D., et al. Dynamic response analysis of a medium-low speed maglev large-span continuous girder bridge under moving vehicle loads. Journal of Railway Science and Engineering, 16(7), 1695–1703, 2019.
4. Wang, B., Zhang, Y., Yu, H., et al. Coupled dynamic response of ultra-high-speed maglev vehicle and simply supported girder bridge. Railway Engineering, 59(8), 5–10, 2019.
5. Han, X., Li, Z., & Chi, M. Influence of guideway beam structure on coupled vibration of medium-low speed maglev vehicle and track. Railway Locomotive & Car, 39(5), 36–42, 2019.
6. Yu, H. Study on influence of maglev guideway stiffness on train running performance. Railway Standard Design, (1), 65–68, 2005.
7. Shi, J. Dynamic response analysis of maglev track beams with different types. *China Sciencepaper*, 7(11), 841-845, 2012.
8. Shi, X. H. *Study on nonlinear dynamic problems of vehicle-track coupling for conventional high-speed maglev trains* [Doctoral dissertation]. National University of Defense Technology, Changsha, 2005.
9. Jiang, Q. L., Zhang, K. L., & Li, X. Digital control of single magnet suspension system. *Journal of the China Railway Society*, 21(A05), 45-48, 1999.
10. Lin, Z. X. *Dynamic analysis of beam-pier-foundation system for maglev suspension system* [Doctoral dissertation]. Shanghai Jiao Tong University, Shanghai, 2003.
11. National Railway Administration of the People's Republic of China. Code for Design of High-Speed Railways: TB 10621-2014[S]. Beijing: China Railway Publishing House, 2015.
12. Standardization Administration of the People's Republic of China. Specifications for Evaluation of Dynamic Performance and Test Authentication of Railway Rolling Stock: GB/T 5599-2019[S]. Beijing: Standards Press of China, 2019.

13. International Union of Railways. UIC518 Testing and approval of railway vehicles from the point of view of their dynamic behavior-safety-track fatigue-running behavior[S]. Paris: International Union of Railway, 2009.